

### A-3.8 Detection of Tropospheric and Polar Stratospheric Clouds for ILAS-type Satellite Sensors

**Contact person** Tatsuya Yokota

Program Research Manager, Center for Global Environmental Research  
National Institute for Environmental Studies, Environment Agency  
16-2 Onogawa, Tsukuba, Ibaraki 305-8506 Japan  
Tel: +81-298-50-2550, Fax: +81-298-58-2645  
E-mail: yoko@nies.go.jp

**EF Fellow name:** Thomas Paul Kurosu

**Total Budget for FY1999 - FY2000** 2,052,000 Yen (FY2000; 1,052,000 Yen)

#### **Abstract**

This study presents a detection method for polar stratospheric clouds (PSCs) from the Environment Agency of Japan's Improved Limb Atmospheric Spectrometer (ILAS) instrument. The PSC detection method is based on ILAS visible channel measurements in and around the oxygen A absorption band (753-784 nm) and involves linear or nonlinear fitting of the spectra to obtain aerosol optical thickness as a function of tangent height. PSC optical thickness is determined from a subsequent linear fit to aerosol optical thickness as a function of altitude. Finally, a fast and simple method for the identification of possible PSC candidates from ILAS measurements is presented.

**Key Words** occultation sensors, nonlinear fitting, transmittance, spectrum, oxygen

#### 1. Introduction

Polar Stratospheric Clouds (PSCs) are a key element in the destruction of ozone in polar atmospheres due to their ability to activate ozone-destroying chlorine reservoirs via catalytic heterogeneous re-actions that occur on their particles in the Polar spring, and the atmospheric denitrification that is associated with their formation. This study presents methods for PSC detection from a satellite sensor ILAS<sup>1)</sup> aboard ADEOS satellite.

During its lifetime from November 1996 until June 1997, ILAS observed a number of PSC events, particularly in the northern hemisphere<sup>2)</sup>. In order to detect PSC presence and to derive their composition, Hayashida *et al.*<sup>2)</sup> used ILAS level-2 data products (aerosol extinction coefficients, volume mixing ratios, etc.) in combination with PSC climatologies. The PSC detection method presented here, on the other hand, is based on ILAS level-1 data (transmittances) in and around the oxygen A absorption band (0.753 - 0.784  $\mu\text{m}$ ). It is thus closer to the operational algorithms developed at NIES, and can provide feedback for the operational aerosol retrieval of ILAS<sup>3-5)</sup>. Furthermore, the PSC detection scheme can easily be adopted to other limb or occultation viewing sensors, such as, for example, the upcoming ILAS-II, ACE or SCIAMACHY<sup>6)</sup> instruments.

#### 2. Research Objective

At the beginning of this research, the research objective was to develop a rapid and effective algorithm for tropospheric and stratospheric PSC detection from ILAS-type limb viewing sensors. However, it was found that tropospheric cloud detection has proven difficult. Due to the large optical thickness of the lower atmosphere, occultation measurements by ILAS terminate around the tropopause level. This makes tropospheric cloud detection

infeasible. Therefore the main objective of this research has been finally dedicated to the stratospheric PSC detection from ILAS-type solar occultation sensors.

### 3. Research Method

PSC detection from ILAS spectra proceeds in three steps, all of which involve linear or nonlinear fitting. They consist of the determination of ILAS instrument parameters, the spectral fitting of ILAS transmittances, and a final fit to aerosol optical thickness as a function of tangent altitude.

#### *Step 1: Determination of instrument parameters*

At tangent altitudes of 100 km or higher virtually no atmospheric extinction is observed, and limb transmission measurements should record a straight line. However, ILAS transmittances at high tangent altitudes show a small tilt as a function of wavelength, which may be attributed to instrument effects. In order to remove such effects, a straight line

$$y(p_0, p_1) = 1.0 + p_0(h) + p_1(h)\lambda, \quad (1)$$

is fitted to ILAS transmittances as a function of wavelength  $\lambda$ , from the topmost tangent height  $h_{\text{top}}$  down to either 110 km or  $h_{\text{top}} - 3$  km, whichever is smaller. The  $p_0(h)$  and  $p_1(h)$  are then averaged over tangent height  $h$ , and, as averaged values  $p_0$  and  $p_1$ , used in Step 2 as input for the spectral fitting.

#### *Step 2: Spectral fitting of ILAS transmittances*

In this step, a model function  $T_h(\lambda)$  is fitted to the transmittances  $T_{h,0}(\lambda)$  as a function of wavelength  $\lambda$  for each observational tangent height  $h$ . The region of oxygen absorption between 0.757 and 0.774  $\mu\text{m}$  is excluded from the fit; the spectral fitting windows are [0.753  $\mu\text{m}$ , 0.757  $\mu\text{m}$ ] and [0.774  $\mu\text{m}$ , 0.784  $\mu\text{m}$ ].

Spectral fitting can be performed using either a linear or a full Levenberg-Marquardt<sup>7)</sup> type nonlinear least-squares fit. Model functions and the actual fitting processes are naturally different for the two approaches. One is a nonlinear fitting uses the following model function:

$$T_h(\lambda) = T_{h,0}(\lambda) \times e^{-\tau_{\text{O}_3}(\lambda)} \times e^{-\tau_{\text{Mie}}/\lambda} \times e^{-\tau_{\text{R}}(\lambda)} - p_0 - p_1\lambda, \quad (2)$$

with  $T_{h,0}(\lambda) = 1$  for occultation transmittances. The model includes contributions from Rayleigh extinction  $\tau_{\text{R}}$ , ozone Wulf band absorption  $\tau_{\text{O}_3}$ , and Mie scattering  $\tau_{\text{Mie}}$  (aerosols and clouds). Note that the  $1/\lambda$  wavelength dependence of Mie scattering is not included in  $\tau_{\text{Mie}}$ . The two instrument parameters  $p_0$  and  $p_1$  from Step 1 are included as well. Only  $\tau_{\text{O}_3}$  and  $\tau_{\text{Mie}}$  are fitted, the other parameters are held fixed for a given tangent height. In particular, Rayleigh optical thickness is computed using the modified UKMO temperature vs. pressure vertical profiles that are also used in ILAS operational processing<sup>2)</sup>. The Rayleigh cross sections are taken from Chance and Spurr<sup>8)</sup>:

Another one is a linear fitting which contains the same fitting parameters  $\tau_{\text{O}_3}$ ,  $\tau_{\text{Mie}}$  (varied), and  $\tau_{\text{R}}$ ,  $p_0$  and  $p_1$  (fixed). However, it requires a preparatory adjustment, in which the instrument baseline is subtracted from the transmittances:

$$\tilde{T}_h(\lambda) = T_h(\lambda) - (p_0 + p_1\lambda). \quad (3)$$

#### *Step 3: Vertical polynomial fit to $\tau_{\text{Mie}}(h)$*

In Step 2, Mie scattering (aerosol) optical thickness  $\tau_{\text{Mie}}$  has been determined from either linear or nonlinear spectral fitting. Since the aim is the detection of PSCs in the ILAS spectra, scenes with increased aerosol optical thickness in the altitude regime of likely PSC formation (~15–30 km) need to be identified. This requires the knowledge of the background aerosol

loading,  $\tau_0(h)$ .  $\tau_0(h)$  is derived from  $\tau_{\text{Mie}}(h)$  by means of a linear polynomial fit as a function of tangent height, excluding the region of PSC formation of  $\sim 15\text{--}30$  km. The model function used for this fit is a polynomial of the following type:

$$\tau_0(\bar{a}, h) = \sum_{i=-6}^1 a_i h^i. \quad (4)$$

Aerosol/PSC optical thickness is determined by subtracting the background values  $\tau_0$  from the total Mie scattering optical thickness  $\tau_{\text{Mie}}$ :

$$\tau_{\text{PSC}}(h) = \tau_{\text{Mie}}(h) - \tau_0(h). \quad (5)$$

#### 4. Results

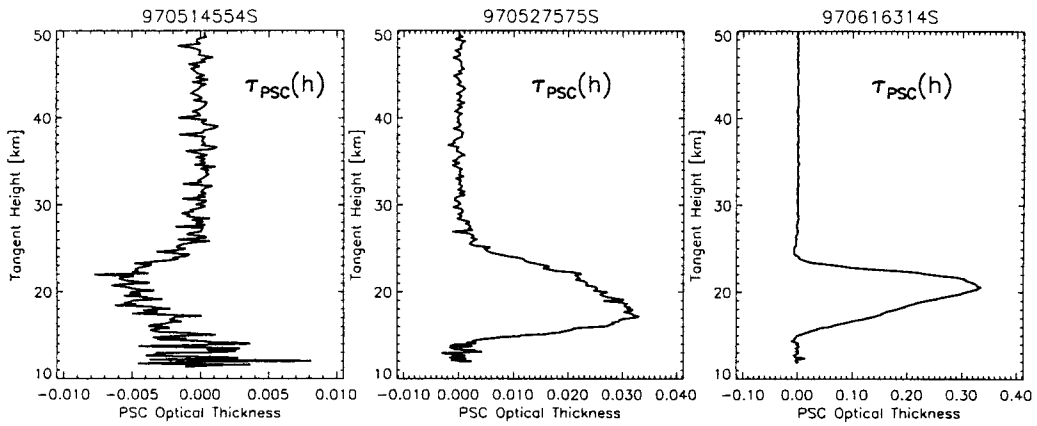


Fig.1 Aerosol/PSC optical thickness  $\tau_{\text{PSC}}(h)$  from Equation (5).

Figure 1 shows  $\tau_{\text{PSC}}$  for the three ILAS observations. The overall small optical thickness in the left panel indicates a “stratospheric background” observation, while enhanced  $\tau$  values in the middle and right panels indicate aerosol and/or PSC presence. This strongly suggests occultation 970616314S to be a PSC event.

#### 5. Discussion

A fast and simple method for the selection of observations that are likely to contain a PSC event are discussed. This method allows a significant reduction of the number of scenes that will be subjected to a more detailed PSC analysis. Such preselection is often important in an operational data processing environment where processing time is critical.

A linear vertical fit to  $\tau_{\text{Mie}}(h)$ , using the model described in Equation (4), was performed under the exclusion of the altitude region of  $\sim 15\text{--}30$  km in order to determine the background values  $\tau_0(h)$ . No use was made of the associated  $\chi^2$ , which shall be denoted as  $\chi^2_{\text{exc}}$  to indicate the exclusion of the PSC altitude region. Performing a similar fit with the same model function but *including* the PSC region will give  $\chi^2_{\text{inc}}$ , with  $\chi^2_{\text{inc}} > \chi^2_{\text{exc}}$  for cases where  $\tau_{\text{Mie}}(h)$  differs significantly from a “background” aerosol loading like 970514554S.

Figure 2 shows a scatterplot “ $\chi^2_{\text{exc}}$  vs  $\chi^2_{\text{inc}}$ ” for  $\chi^2$  values from two vertical linear fits to  $\tau_{\text{Mie}}$  according to Equation (4). Each pair of  $\chi^2$  values is represented by a black triangle. The dashed lines mark the (empirically determined) equality

$$\chi^2_{\text{inc}} = 0.3 \times [\chi^2_{\text{exc}}]^{1/2}. \quad (6)$$

The light-grey triangles indicate all those pairs of  $\chi^2_{\text{inc}}(\tau_{\text{Mie}})$  and  $\chi^2_{\text{exc}}(\tau_{\text{Mie}})$  for which

$$\chi^2_{\text{inc}}(\tau_{\text{Mie}}) \geq 0.3 \times [\chi^2_{\text{exc}}(\tau_{\text{Mie}})]^{1/2}. \quad (7)$$

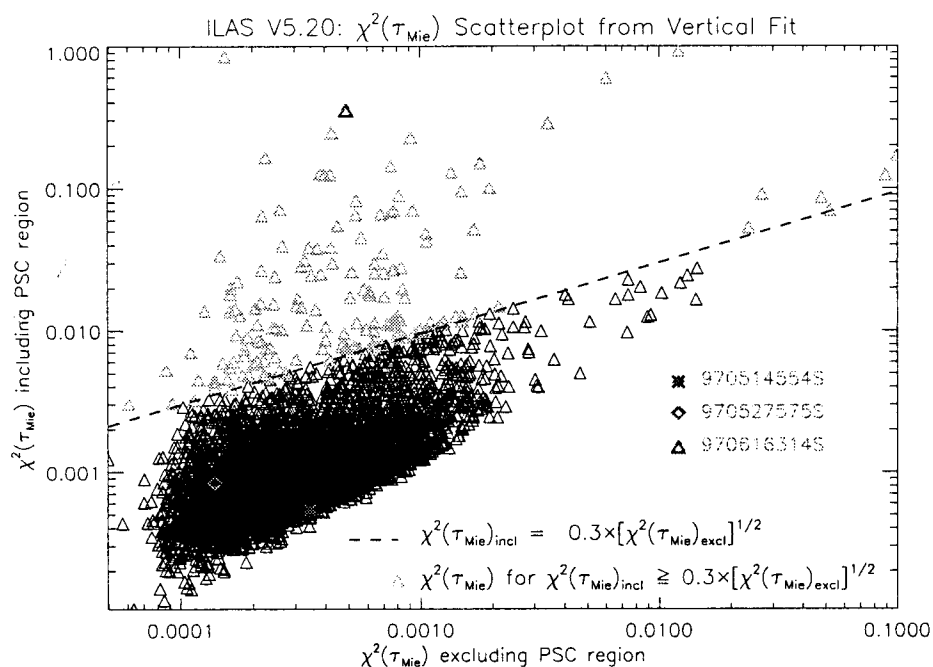


Fig.2 Scatterplot “ $\chi^2_{exc}$  vs  $\chi^2_{inc}$ ” for  $\chi^2$  values from two linear vertical fits to using the model function from Equation (4), including and excluding altitudes of likely PSC occurrence.

Figure 2 also contains the three case studies, indicated by dark-grey plot symbols. The figure shows that using the selection criterion of Equations (6) and (7) can significantly reduce the number of observations that will be subjected to further PSC processing.

### References

- 1) Sasano, Y., M. Suzuki, T. Yokota, and H. Kanzawa, Improved Limb Atmospheric Spectrometer (ILAS) for stratospheric ozone layer measurements by solar occultation technique, *Geophysical Research Letters*, **26**(2), 197–200 (1999).
- 2) Hayashida, S., N. Saitoh, A. Kagawa, T. Yokota, M. Suzuki, H. Nakajima, and Y. Sasano, Arctic polar stratospheric clouds observed with the improved limb atmospheric spectrometer during the winter of 1996/1997, *Journal of Geophysical Research*, **105**(D20), 24,715–24,730 (2000).
- 3) Dubovik, O., T. Yokota, and Y. Sasano, Improved technique for data inversion and its applications to the retrieval algorithm for ADEOS/ILAS, *Advances in Space Research*, **21**(3), 397–403 (1998).
- 4) Okamoto, H., Y. Sasano, S. Mukai, I. Sano, H. Ishihara, T. Matsumoto, L. Thomason, and M. Pitts, ADEOS/ILAS aerosol retrieval algorithm with 5 channels, *Advances in Space Research*, **21**(3), 443–446 (1998).
- 5) Yokota, T., M. Suzuki, O. Dubovik, and Y. Sasano, ILAS (Improved Limb Atmospheric Spectrometer)/ADEOS data retrieval algorithms, *Advances in Space Research*, **21**(3), 393–396 (1998).
- 6) Bovensmann, H., J. Burrows, M. Buchwitz, J. Frerick, S. Noel, V. Rozanov, K. Chance, and A. Goede, SCIAMACHY: Mission objectives and measurement modes, *Journal of the Atmospheric Sciences*, **56**, 127–150 (1999).
- 7) Marquardt, D., *J. Soc. Indust. Appl. Math.*, **11**, 431 (1963).
- 8) Chance, K. V. and R. J. Spurr, Ring effect studies: Rayleigh scattering including molecular parameters for rotational Raman scattering, and the Fraunhofer spectrum, *Applied Optics*, **36**(21), 5224–5230 (1997).